

Forum

Investigating Metalloenzyme Reactions Using Electrochemical Sweeps and Steps: Fine Control and Measurements with Reactants Ranging from Ions to Gases

Kylie A. Vincent and Fraser A. Armstrong*

Department of Chemistry, Inorganic Chemistry Laboratory, University of Oxford, South Parks Road, Oxford OX1 3QR, England

Received October 21, 2004

Protein film voltammetry is a powerful method for probing the chemistry of redox-active sites in metalloproteins. The technique affords precise potential control over a tiny quantity of material that is manipulated on an electrode surface, providing information on ligand- or metal-exchange reactions coupled to electron transfer. This is illustrated by examples of transformations of the iron–sulfur clusters in ferredoxins. Protein film voltammetry is particularly advantageous in studies of metalloenzymes for which the current response is proportional to catalytic activity: kinetic data of extremely high signal/noise ratio are obtained for highly active enzymes. We present a series of interesting examples in which catalytic activity varies in unusual ways with applied potential, surveying information that can be obtained from cyclic voltammetry and then looking beyond this method to controlled potential-step experiments that yield kinetic and mechanistic details. Recent results on the voltammetry of the highly active [NiFe]-hydrogenase from *Allochromatium vinosum* illustrate how it is possible to use the precise kinetic information from potential-step experiments to diagnose subtle details of transformations between catalytically active and inactive states of an enzyme. Protein film voltammetry thus complements spectroscopic techniques and other physical methods, revealing the chemistry of systems that might appear intractable or convoluted by other means.

Introduction

Direct, dynamic electrochemical methods are becoming established for investigating redox-active metal centers in proteins, and we and others have advocated the advantages of immobilizing the protein on an electrode (Figure 1) rather than having the molecules free in solution.^{1–3}

Indeed, many interesting properties of redox proteins and their active sites, otherwise hidden or intractable, are revealed by applying the concept and techniques we refer to as “protein film voltammetry” (PFV). Contrary to the general opinions held more than a decade ago, there is little doubt

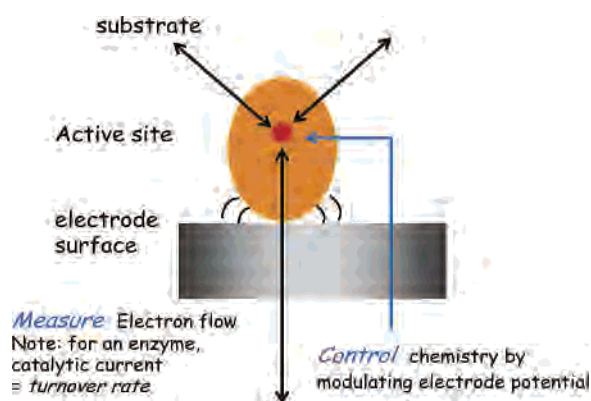
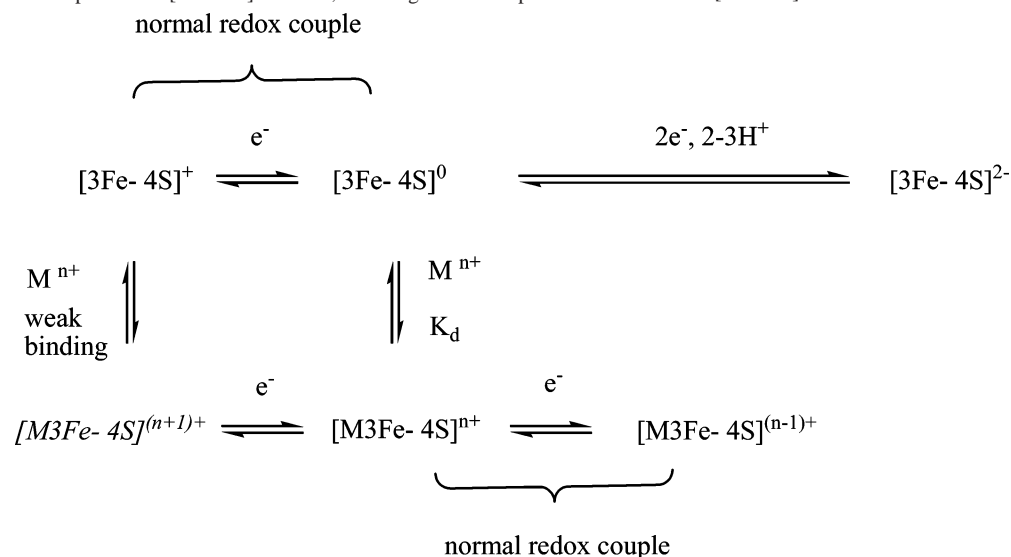


Figure 1. Cartoon showing an enzyme anchored to an electrode surface so that its active sites are controlled by the electrode potential and its activity is measured through the catalytic current.

that metal centers in proteins can undergo rapid, reversible electron exchange with an electrode (a key factor being the

* To whom correspondence should be addressed. E-mail: fraser.armstrong@chem.ox.ac.uk.

- (1) Léger, C.; Elliott, S. J.; Hoke, K. R.; Jeuken, L. J. C.; Jones A. K.; Armstrong, F. A. *Biochemistry* **2003**, *42*, 8653.
- (2) Armstrong, F. A.; Heering, H. A.; Hirst, J. *Chem. Soc. Rev.* **1997**, *26*, 169.
- (3) Armstrong, F. A.; Wilson, G. S. *Electrochim. Acta* **2000**, *45*, 2623.

Scheme 1. Metal Ion Uptake into [3Fe-4S] Clusters, Showing Favored Uptake of M^{n+} into the [3Fe-4S]⁰ State


typically small reorganization energy of protein electron-transfer sites), and even a deeply buried center can register fast electron transfer if there is a relay system of hemes or Fe-S clusters leading to the surface where contact is made with the electrode. The challenge is therefore to design the electrode surface for binding a particular protein tightly and in the correct orientation for optimal electron transfer. Studies so far have focused mainly on cyclic voltammetry, which is the electrochemical technique most widely used by inorganic chemists, albeit mainly as a qualitative tool.⁴ Cyclic voltammetry has been exploited to study a wide range of metalloproteins, providing unique information on reactions coupled to electron transfer and the often subtle effects of ligand, metal, or amino acid substitutions on reactivity. For redox enzymes, cyclic voltammetry has also provided unusual insight into the potential dependence of catalytic activity and the effects of inhibitors and activators. This paper seeks to summarize the concepts illustrated by cyclic voltammetry and then look beyond this technique to describe the kinetic and mechanistic information that can be derived from potential-step methods. We outline how the electrochemistry of a protein in an adsorbed film is used to elucidate the redox chemistry of its active sites, and we present recent data obtained for a [NiFe]-hydrogenase as an example of how it is possible to diagnose important yet subtle details of complex enzyme transformations.

Background

An early success of protein film voltammetry was the elucidation of reactions of labile Fe-S clusters.⁵ There are now many examples of proteins that contain a functionally unstable Fe-S cluster, i.e., a center that in nature is intended to vacillate between different structures depending on potential, metal ion availability (Fe, of course, and other

metals), and pH. These include the first such example, aconitase, and subsequent discoveries such as the iron regulatory protein (cytosolic aconitase), various Fe-S “sensory” transcription factors, and proteins required for Fe-S cluster assembly.⁶ Our story begins with a small, unstable ferredoxin (FdIII) from *Desulfovibrio africanus*, which contains one [4Fe-4S] cubane and one [3Fe-4S] cuboidal cluster.^{7,8} At first glance, this protein might appear to have little of interest, but during EPR spectroscopic studies, it was noted that the amount of [3Fe-4S] cluster was difficult to quantify and varied greatly between different samples. The fact, as it emerged, was that, upon reduction with dithionite, the [3Fe-4S] cluster was rapidly sequestering trace Fe (including Fe released by protein degradation) and converting into a second [4Fe-4S] cluster in which the added Fe is coordinated by a noncysteine ligand. The chemistry is summarized in Scheme 1, which shows the separate processes of electron transfers and chemical transformations in the horizontal and vertical directions, respectively. The overall reaction, depicted in Figure 2A, is analogous to the activation of aconitase, where the labile Fe is the site of substrate binding.

In solution, the reaction in Scheme 1 proved very difficult to control, and the situation was complicated further because, as is usually the case for Fe-S proteins displaying only overlapping broad bands in the visible spectrum, one had little idea of cluster composition until the solution was freeze-quenched and the EPR spectrum measured. An improvement was on hand when the cyclic voltammetry of a solution of FdIII (Figure 2B), measured using a pyrolytic graphite “edge” (PGE) electrode, revealed the two clusters as redox couples, each at the expected potential. The relative size of the signal at high potential (I) due to [3Fe-4S]⁺⁰ when compared to the one at lower potential due to [4Fe-4S]^{2+/+} (II) provided

(4) Bard, A. J.; Faulkner, L. R. *Electrochemical Methods: Fundamentals and Applications*; Wiley: New York, 2001.

(5) Armstrong, F. A. In *Electroanalytical Methods of Biological Materials*; Brajter-Toth, A., Chambers, J. Q., Eds.; Marcel Dekker: New York, 2002; pp 143–194.

(6) Kiley, P. J.; Beinert, H. *Curr. Opin. Microbiol.* **2003**, *6*, 181–185.

(7) Armstrong, F. A.; George, S. J.; Cammack, R.; Hatchikian E. C.; Thomson, A. J. *Biochem. J.* **1989**, *264*, 265–273.

(8) George, S. J.; Armstrong, F. A.; Hatchikian, E. C.; Thomson, A. J. *Biochem. J.* **1989**, *264*, 275–284.

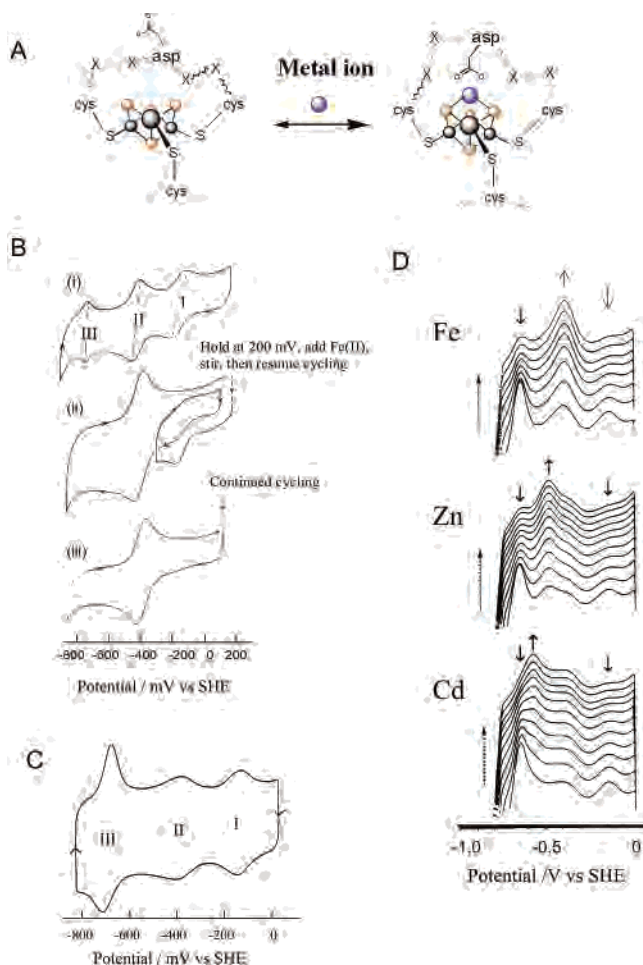


Figure 2. Transformations of an Fe-S cluster in a protein as revealed by cyclic voltammetry. (A) Interconversion between $[3\text{Fe}-4\text{S}]$ and $[\text{M}3\text{Fe}-4\text{S}]$ clusters in the small ferredoxin (FdIII) from *Desulfovibrio africanus*. It is unclear whether the carboxylate side chain of Asp coordinates to the cluster. (B) Cyclic voltammetry of a solution of FdIII (at a PGE electrode) showing (top) signals due to stable $[4\text{Fe}-4\text{S}]$ (II) and reactive $[3\text{Fe}-4\text{S}]$ (I, III) clusters, followed by (middle) addition of Fe(II) to the cell solution, and (bottom) the voltammogram resulting after many slow cycles (16 mV s^{-1}). (C) Voltammogram of a film of FdIII formed on a PGE electrode, showing how clear sharp signals are obtained from less than a picomole of immobilized protein at 1 V s^{-1} . (D) Changes in signals as the FdIII-coated electrode is placed into solutions containing Fe, Zn, or Cd at a scan rate of 0.5 V s^{-1} . (Adapted from ref 11)

an approximate guide as to the quantity of each cluster present. However, observing signal I required slow scan rates, and the electrode did not prevent species far from the electrode (and thus out of potential control) from undergoing seemingly chaotic Fe uptake.

The breakthrough came when it was discovered that, by applying just a tiny amount of ferredoxin solution containing a polyamine such as neomycin, to the surface of the PGE electrode, strong signals were obtained from just a molecular layer of protein (Figure 2C); these signals remained sharp at scan rates well above 1 V s^{-1} .⁹ The polyamine acts as a coadsorbate to stabilize the film by forming electrostatic interactions between the negatively charged ferredoxin and the oxide-rich graphite electrode surface. Because complicated and sluggish protein diffusion was not involved, the

area under each peak provided a much better guide as to the number of active sites being addressed and their relative stoichiometries in a multicentered protein. The technique established a new redox couple, the unusual, cooperative two-electron reduction of $[3\text{Fe}-4\text{S}]^0$ coupled to proton uptake (signal III), which has since been identified in many other small proteins and enzymes. The signal integrates to twice the charge of the signal due to $[3\text{Fe}-4\text{S}]^{+/0}$ and is sharp because a cooperative two-electron transfer produces a peak that is one-half the width and four times the height of a one-electron reaction.⁹ Despite the absence of a full spectroscopic characterization of the hyper-reduced state, the pair of signals (the equivalent of I and III in different proteins) provides a signature for the presence of a $[3\text{Fe}-4\text{S}]$ cluster.¹⁰

When the PGE electrode with the film of FdIII was introduced into a solution containing Fe(II), it was easy to observe and control the reaction taking place. Upon cycling to potentials below the value for the $[3\text{Fe}-4\text{S}]^{+/0}$ redox couple (signal I), the signals due to $[3\text{Fe}-4\text{S}]^{+/0}$ and $[3\text{Fe}-4\text{S}]^{0/2-}$ (I and III) disappear simultaneously with the appearance of a new signal due to the new $[4\text{Fe}-4\text{S}]^{2+/+}$ redox couple. Using orders of magnitude less sample than the amount required to measure an EPR spectrum (the electrode is coated with less than a picomole of protein), it proved possible to make extensive studies of uptake and release not only of Fe, but also of other metals (Figure 2D).¹¹⁻¹⁵ In all cases, the cubane product operates as a $2+/+$ redox couple. The affinities (K_d) of different divalent metals for the $[3\text{Fe}-4\text{S}]^0$ core were measured by holding the potential to lock the $[3\text{Fe}-4\text{S}]^0$ state and then cycling rapidly to observe the extent of transformation. For Tl^+ , the transformation in either direction is so rapid (Tl^+ binds also to the $[3\text{Fe}-4\text{S}]^+$ state, albeit weakly) that values of K_d for both oxidized ($[\text{Tl}3\text{Fe}-4\text{S}]^{2+}$) and reduced ($[\text{Tl}3\text{Fe}-4\text{S}]^+$) clusters were determined from the positive shift in potential for signal I.¹² The reduction potentials of the various $[\text{M}3\text{Fe}-4\text{S}]^{2+}$ products ($\text{M} = \text{Fe}, \text{Co}, \text{Zn}, \text{Cu}, \text{Cd}, \text{Tl}$) reflect the different stabilizations afforded by reduction to $[\text{M}3\text{Fe}-4\text{S}]^+$, which can release M^+ (this is easy for the Tl adduct) but cannot release M^{2+} without forming an unstable oxidation level ($1-$) of the $[3\text{Fe}-4\text{S}]$ product (like $[\text{Tl}3\text{Fe}-4\text{S}]^{2+/+}$, the $[\text{Cu}3\text{Fe}-4\text{S}]^{2+/+}$ cluster has a high reduction potential; the Cu is bound as Cu(I)). Further studies were carried out on various proteins containing $[4\text{Fe}-4\text{S}]$ clusters to examine their degradation upon application of high-potential pulses. Here, it was possible to observe the signals due to the $[3\text{Fe}-4\text{S}]$ cluster, formed as a relatively stable product of oxidative damage.¹⁶

(9) Armstrong, F. A.; Butt, J. N.; George, S. J.; Hatchikian, E. C.; Thomson, A. J. *FEBS Lett.* **1989**, *259*, 15-18.

(10) Duff, J. L. C.; Breton, J. L. J.; Butt, J. N.; Armstrong, F. A.; Thomson, A. J. *J. Am. Chem. Soc.* **1996**, *118*, 8593-8603.
 (11) Butt, J. N.; Armstrong, F. A.; Breton, J.; George, S. J.; Thomson, A. J.; Hatchikian, E. C. *J. Am. Chem. Soc.* **1991**, *113*, 6663-6670.
 (12) Butt, J. N.; Sucheta, A.; Armstrong, F. A.; Breton, J.; Thomson, A. J.; Hatchikian, E. C. *J. Am. Chem. Soc.* **1991**, *113*, 8948-8950.
 (13) Butt, J. N.; Niles, J.; Armstrong, F. A.; Breton, J.; Thomson, A. J. *Nat. Struct. Biol.* **1994**, *1*, 427-433.
 (14) Butt, J. N.; Fawcett, S. E. J.; Breton, J.; Thomson, A. J.; Armstrong, F. A. *J. Am. Chem. Soc.* **1997**, *119*, 9729-9737.
 (15) Fawcett, S. E. J.; Davis, D.; Breton, J. L.; Thomson, A. J.; Armstrong, F. A. *Biochem. J.* **1998**, *335*, 357.
 (16) Tilley, G. J.; Camba, R.; Burgess, B. K.; Armstrong, F. A. *Biochem. J.* **2001**, *360*, 717-726.

The concept of “potential control” was thus demonstrated to be an important factor in studying and understanding these reactions.

The experiments also allow numerous rapid transfers of a single protein sample between electrolytes containing different reactants. This provided a new way to investigate protonation equilibria at the Rieske [2Fe–2S] center in the bc_1 respiratory complex.¹⁷ The Rieske center has bis-imidazole coordination to one of the Fe atoms, and deprotonation of one or both of these ligands results in a pH-dependent reduction potential. Hirst and co-workers studied the soluble Rieske fragment from the bc_1 complex of *Thermus thermophilus*. The fact that the protein is adsorbed as a film allowed studies to be made over a very wide range of pH, up to pH 14 (the protein is remarkably robust). Although far from having any direct physiological significance, this “extrapolative” procedure allowed a remarkably detailed potential–pH plot to be constructed (pH 3–14), revealing different pK values and showing that the doubly deprotonated state formed just above pH 12, in which both imidazoles have probably become anionic donors, has a low reduction potential that is more in line with normal all-thiolate (RS^-) ligation.

Numerous efforts have been made to extend the ways in which proteins can be immobilized on electrodes: successes have included pyrolytic graphite edge (PGE), graphite modified with surfactant films, conducting metal oxides, and gold surfaces modified with a variety of self-assembled organo-thiol monolayers designed to bind the protein of interest.³ It must be stated that our knowledge of the landscape of the protein–electrode interface is currently quite unsatisfactory, yet we have managed to exploit the fact that whatever the structure or dynamics, electron transfer is usually faster than the chemistry we wish to study. One argument frequently posed against studying a protein bound tightly on an electrode is that it is a rather *unnatural* environment. The counterargument of course is that proteins are very commonly associated with biological surfaces (membranes) and it would be naïve to believe that a dilute solution in buffer (or even worse frozen) is any better approximation to the truth. Another persuasive aspect is that, whereas a small molecule, surrounded by solvent, is almost certain to have altered properties when attached to an electrode, the same is unlikely to be true of an active site that is well buried and shielded within a protein molecule that can be more than 100 Å in diameter.

Voltammetric Signals Provide Kinetic Information

In cyclic voltammetry performed on a protein film, two classes of “signal” are observed.^{1,2} The first case is a “nonturnover” signal, which reports on electrochemically cycled electron transfer: the electron enters the active site (producing the reduction peak) and is then returned to the electrode (producing the oxidation peak) as the potential is cycled. The potentials and shapes (widths, symmetry) of the

reduction and oxidation peaks provide important information on inherent rates of electron transfer; coupled reactions such as proton transfer; and properties of the sample as a whole, such as number and homogeneity of active sites in the film. We have just seen an example of this in Figure 2.

Figure 3 shows an example in which the focus of interest is the mechanism of a long-range proton-coupled electron-transfer process. In this case, the full study, which included a detailed program of site-directed mutagenesis and crystallography, revealed the mechanism of proton transfer in a protein at atomic resolution.¹⁸ The subject was a buried [3Fe–4S] cluster in a small ferredoxin (FdI) from *Azotobacter vinelandii*, unusual in that the reduced ([3Fe–4S]⁰) form binds a proton at neutral pH (the pK is around 8). The proton probably binds to a μ_2 -S atom and might distribute itself among all three sites.¹⁹ The structure of the protein has been solved to high resolution with the [3Fe–4S] cluster in different oxidation states and at high and low pH. The region between the [3Fe–4S] cluster and the protein surface is shown in Figure 3A. Once again, the protein adsorbs to high coverage at a PGE electrode (approximately as expected for a monolayer). For understanding the electrochemistry, we need only consider the information that is afforded by taking *any* system in which rapid electron transfer to an active site is followed by proton transfer, while the reverse reaction requires that proton transfer occurs before electron transfer. In Scheme 2, these reactions are depicted as two sides of a thermodynamic square scheme, and in electrochemical terminology, the overall reduction and reoxidation is known as an “ECCE” reaction [E = electrochemical step (horizontal), C = chemical step (vertical)]. Here, k_0 is the electrochemical exchange rate constant, and k_{on} and k_{off} are the rate constants for proton transfer to and from the cluster, respectively.

As the scan rate is increased, the signal changes systematically, as shown in Figure 3B, in ways that depend on pH. The overall picture is represented in a “trumpet plot”, Figure 3C, which displays how each peak position varies with the scan rate (plotted in logarithmic form).²⁰ The results shown are for a slow mutant (D15N) in which an aspartic acid whose carboxylate carries the proton in and out of the protein has been replaced by asparagine. This acid-to-amide mutation is a common strategy for determining whether a particular carboxylate side chain is involved in proton transfer. At sufficiently low rate, the signal in either case consists of a pair of peaks centered at the reduction potential for the overall reaction. This is analogous to carrying out a potentiometric measurement. For $pH > pK$, the reaction consists only of electron transfer and the separation of peaks with increasing scan rate yields the rate constant k_0 . For the condition $pH < pK$, two *kinetic* regions are distinguished. First, in the “gated ET region”, the rate of the return sweep exceeds the *proton-off* rate; the electron is trapped, and the

(17) Zu, Y. B.; Fee, J. A.; Hirst, J. *J. Am. Chem. Soc.* **2001**, *123*, 9906–9907.

(18) Chen, K. S.; Hirst, J.; Camba, R.; Bonagura, C. A.; Stout, C. D.; Burgess, B. K.; Armstrong, F. A. *Nature* **2000**, *405*, 814–817.

(19) Bentrop, D.; Bertini, I.; Borsari, M.; Cosenza, G.; Luchinat, C.; Niikura, Y. *Angew. Chem., Int. Ed.* **2000**, *39*, 3620–3622.

(20) Hirst, J.; Duff, J. L. C.; Jameson, G. N. L.; Kemper, M. A.; Burgess, B. K.; Armstrong, F. A. *J. Am. Chem. Soc.* **1998**, *120*, 7805–7094.

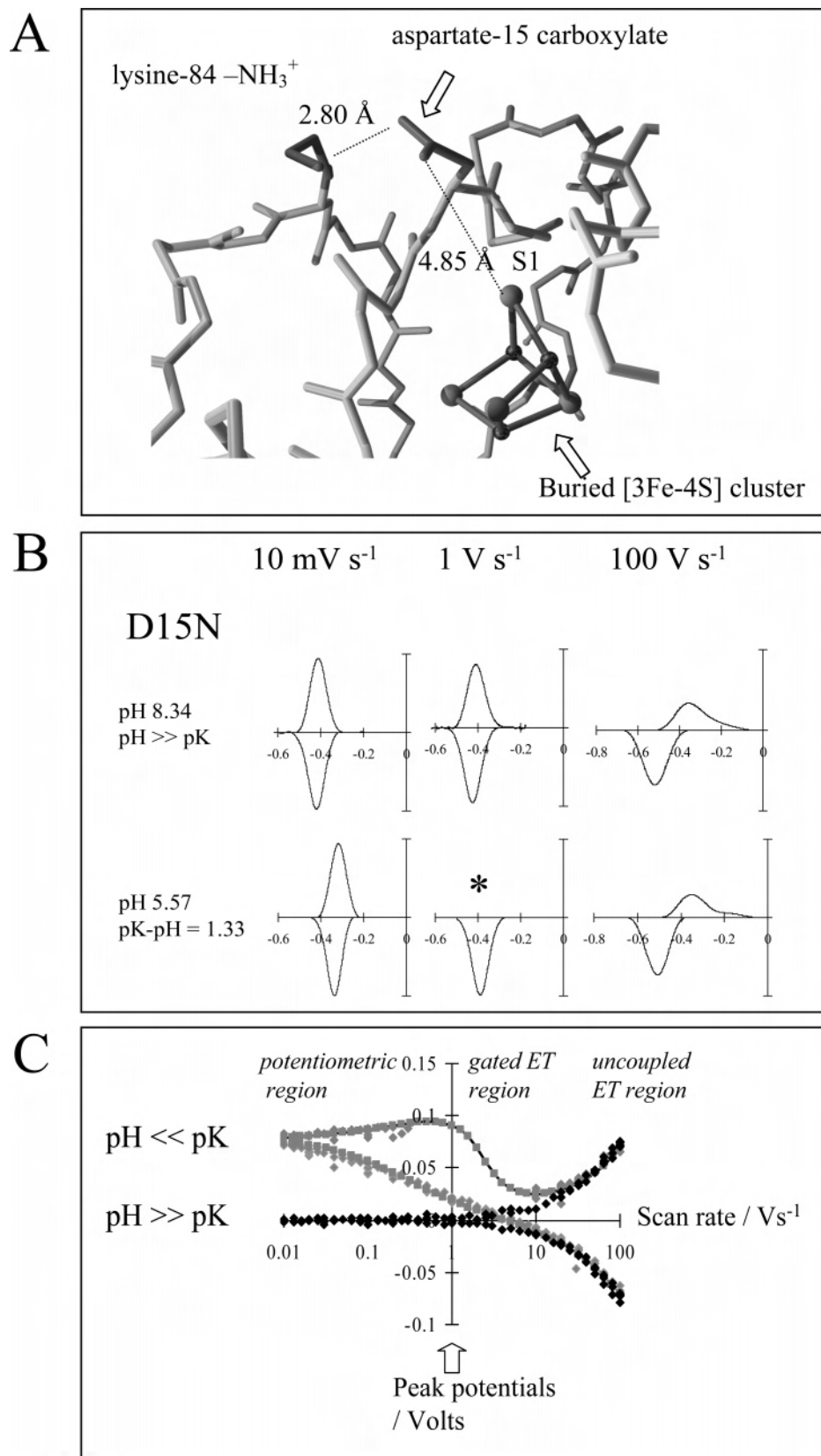
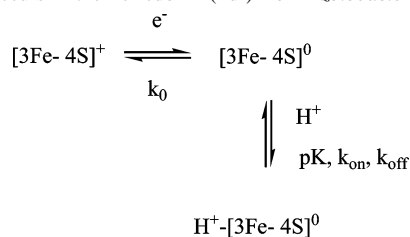


Figure 3. (A) Structure of the region of interest for long-range proton transfer in *Azotobacter vinelandii* FdI showing the buried [3Fe-4S] cluster and the position of the carboxylate side chain from aspartate-15. (B) Voltammograms for a film of the D15N mutant of *Azotobacter vinelandii* FdI at pH 8 and 5, at increasing scan rates. Temperature = 0 °C. At pH 8.5, no proton transfer occurs. At pH 5, proton transfer occurs, but in the mutant, it is sufficiently slow that reoxidation appears blocked at 1 V s^{-1} and there is no time for the proton to transfer to the cluster at 100 V s^{-1} . (Adapted from ref 20.) (C) Trumpet plots showing variation of oxidative and reductive peak positions with scan rate and the three kinetic regions (time domains) that are distinguished by the experiment. The plots are analyzed to yield the kinetics and mechanism of proton transfer. In this case, for the D15N mutant, the proton-off rate is just 2.5 s^{-1} .

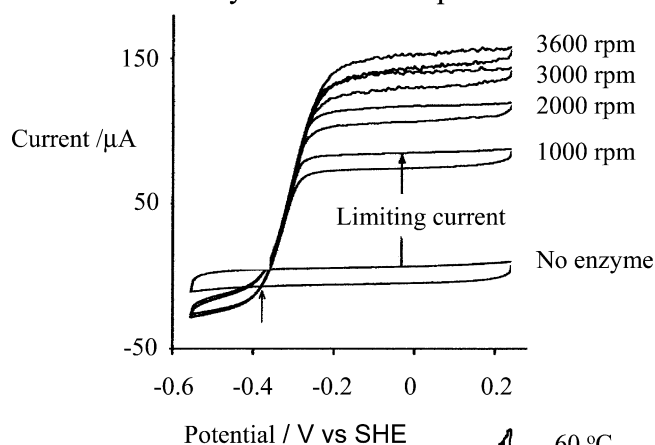
Scheme 2. Proton-Coupled Electron Transfer at a $[3\text{Fe}-4\text{S}]^{+0}$ Cluster as Occurs in the Ferredoxin (FdI) from *Azotobacter vinelandii*

oxidation peak is lost. Then, at sufficiently high scan rate, in the “uncoupled ET region”, the oxidation peak reappears as the potential is reversed before the proton can bind; note that the peaks for $\text{pH} \gg \text{pK}$ and $\text{pH} \ll \text{pK}$ now coincide, so that, on this time scale (below 10 ms), the reduction potential becomes independent of pH. By mutating different residues in the protein, a wealth of detailed information on proton transfer, redox energetics, and electrostatics was obtained, and these data have continued to form a basis for discussions on proton-transfer mechanisms.^{21–23} We will not discuss these results further, but emphasize that the data, a combination of kinetics and energetics, are difficult if not impossible to obtain by other means.

Catalytic Voltammograms of Enzymes

The other class of voltammetric signal is the catalytic wave, which reports on the activity of an enzyme that is confined as a film. Here, we note the amplitude of the wave, for which the current translates directly into turnover rate. The position and shape of the wave inform us about the potential that drives an event (such as a particular redox process in the enzyme that is crucial for catalytic action) and whether electron transfer is rate-determining (and if so, how many electrons are involved in the transition state). It is easily argued that a cyclic voltammogram displaying “perfect” behavior, i.e., showing peaks that are as expected for a fully reversible, diffusion-controlled reaction, merely informs us of the reduction potential of a boring compound that does little but shuttle electrons. The same can be said for the “textbook” sigmoidal catalytic voltammogram of an enzyme film, although interesting features are often revealed upon closer interrogation. The voltammograms shown in Figure 4 are examples of experiments that do not reveal very much about the active sites but do shed light on the factors controlling the electrochemical reactions. Figure 4A shows the voltammetry displayed by molecules of a $[\text{NiFe}]$ -hydrogenase (from the purple bacterium *Allochromatium vinosum*) adsorbed at a rotating disk PGE electrode, catalyzing H_2 oxidation (0.1 bar H_2).²⁴ This enzyme is extremely electroactive and consumes H_2 at rates well over 1000 s^{-1} (see later). The film was formed by adsorption from dilute

A Control by substrate transport



B

Control by interfacial electron transfer (dispersed)

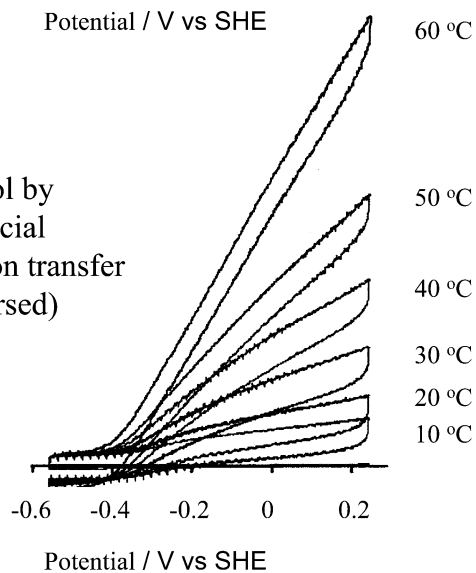


Figure 4. Voltammograms of the $[\text{NiFe}]$ -hydrogenase from *Allochromatium vinosum*, adsorbed at a PGE electrode, with experiments operating under different conditions: (A) Under conditions of H_2 mass-transport control, pH 6.5, 0.1 bar H_2 , 30 °C, scan rate = 100 mV s^{-1} , electroactive coverage $< 3 \text{ pmol cm}^{-2}$. Various electrode rotation rates. (Adapted from ref 24.) (B) Under conditions revealing the transition to electron-transfer control as the temperature is raised. Scan rate = 1 V s^{-1} , electrode rotation rate = 1500 rpm, pH 7.0, electroactive coverage $\ll 3 \text{ pmol cm}^{-2}$. (Adapted from ref 25.)

solution, followed by washing and placement in a sealed cell. At a scan rate of 0.2 V s^{-1} , H_2 oxidation is observed as a large sigmoidal wave that increases in magnitude with the square root of the rate of electrode rotation. This is diagnostic of an electrode reaction that is controlled by mass transport of the substrate to the electrode surface; the relevant mathematical relationship is the Levich equation.

To help alleviate the restriction of diffusion control, we can lower the coverage of enzyme on the surface; for example, the electrode can even be polished gently *after* formation of a film. Lowering the coverage of catalyst causes the waveform to become independent of the rotation rate. Figure 4B illustrates a striking effect of temperature on the catalytic waveform observed for the same $[\text{NiFe}]$ -hydrogenase.²⁵ At low temperature, a sigmoidal wave is observed that can be explained in terms of the rate-determining step

(21) Camba, R.; Jung, Y.-S.; Hunsicker-Wang, L. M.; Burgess, B. K.; Stout, C. D.; Hirst, J.; Armstrong, F. A. *Biochemistry* **2003**, *42*, 10589–10599.

(22) Cherepanov, D. A.; Mulikidjanian, A. Y. *Biochim. Biophys. Acta* **2001**, *1505*, 179–184.

(23) Meuwly, M.; Karplus, M. *Biophys. J.* **2004**, *86*, 1987–2007.

(24) Pershad, H. R.; Duff, J. L. C.; Heering, H. A.; Duin, E. C.; Albracht S. P. J.; Armstrong, F. A. *Biochemistry* **1999**, *38*, 8992.

(25) Léger, C.; Jones, A. K.; Albracht, S. P. J.; Armstrong, F. A. *J. Phys. Chem. B* **2002**, *106*, 13058.

being the reaction at the active site, which becomes independent of potential as soon as electrons are supplied at a sufficient rate to sustain catalytic demand. As the temperature is raised, the waveform becomes linear. The behavior is reminiscent of an ohmic resistor, but the origin is more likely the nonideality of the adsorbed enzyme film due to enzyme molecules adopting various orientations with respect to the electrode surface that they contact. At the higher temperatures, electron transfer becomes rate-limiting (the activation energy for electron transfer is lower than for the reactions at the active site), but rather than there being a single rate constant for interfacial exchange, the range of enzyme orientations leads to a wide dispersion. This produces a range of systems that obey Marcus theory, and the linear behavior can be modeled. To study the [NiFe] active site of hydrogenases by dynamic electrochemical methods, it is therefore important to ensure that the enzyme controls the action.

Information from the Potential Dependence of Catalytic Activity. Most redox enzymes catalyze two-electron reactions. Because of the presence of a multiple-electron active site and one or more electron relay centers, they can also exist in several complex oxidation levels. It should not be surprising therefore that the activity of a redox enzyme can be fine-tuned so that it depends *critically* upon the potential that is applied rather than following the simple driving force requirement (by this we mean the higher the driving force, the faster the reaction). An early example of this came to light with studies on beef heart mitochondrial succinate dehydrogenase, which is an Fe–S flavoenzyme that catalyzes the oxidation of succinate to fumarate at a potential of around 0 mV.²⁶ A water-soluble membrane-extrinsic subcomplex known as SdhAB can be prepared that contains the active site flavin and three Fe–S clusters as a relay. Succinate dehydrogenase is known to work in reverse; so when a PGE electrode modified by adsorption of SdhAB was cycled in a solution of fumarate, we were surprised to observe that the current due to fumarate reduction drops sharply below a certain value despite the increasing driving force. Figure 5A shows experiments in which SdhAB is catalyzing the interconversion of a 1:1 mixture of fumarate and succinate, either with normal substrates (H) or fully deuterated (D) substrates (see below).²⁷ We have termed the attenuation of activity the “tunnel diode effect” because it resembles the electronic device that displays *negative* resistance in a certain potential region; in other words, the current drops as the bias increases. This kind of behavior has now been observed for many enzymes.²⁸ It can arise for various reasons: an intermediate redox state might be the most active in some crucial point of the catalytic cycle (for example, it might be that the substrate binds much more tightly to the intermediate redox state, such as the flavin

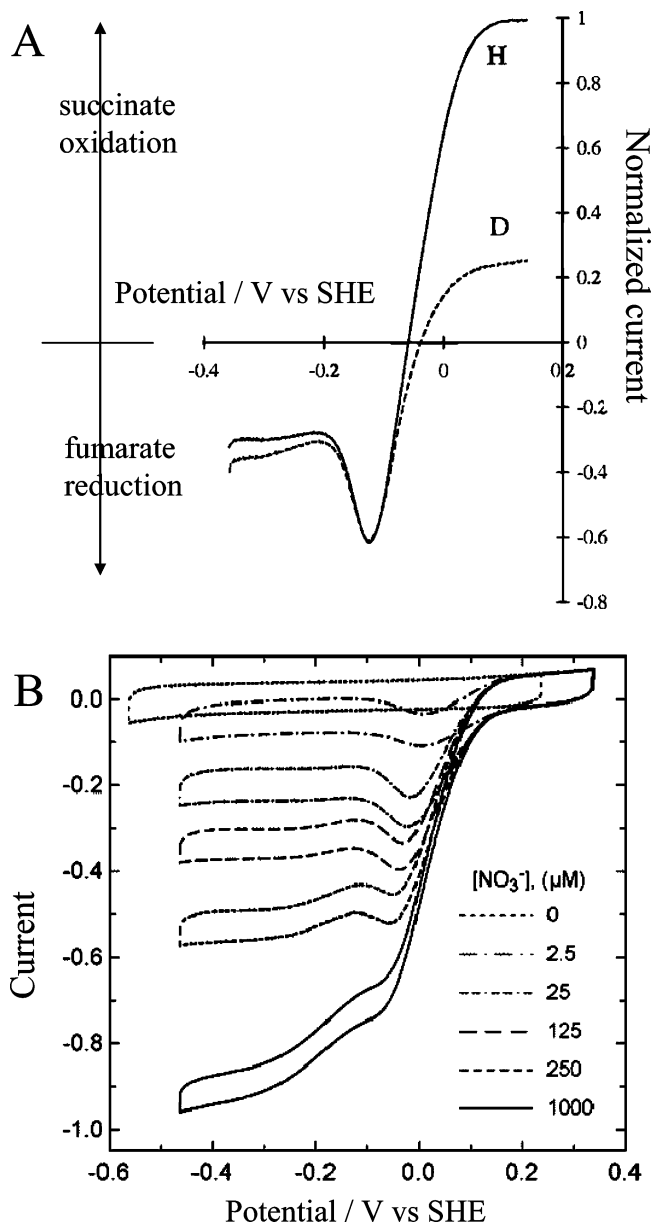


Figure 5. Voltammograms showing the unusual potential dependence of catalytic activity of different oxidoreductases adsorbed on a PGE electrode. (A) Succinate dehydrogenase (SdhAB from beef heart mitochondria) catalyzing interconversion of H/D fumarate and succinate, each at 5 mM concentration in the cell, pH 7.8, temperature = 38 °C, scan rate = 10 mV s⁻¹, electrode rotation rate = 400 rpm. (Adapted from ref 27.) (B) Nitrate reductase (NarGHI from *E. coli*), pH 7.0, temperature 30 °C, scan rate 10 mV s⁻¹, electrode rotation rate = 2100 rpm. Various concentrations of nitrate, as shown. (Adapted from ref 31.)

radical); alternatively, application of a potential that is too oxidizing or too reducing causes the active site to revert to a completely inactive form, in which case the exact forms of the voltammograms depend on the kinetics of the inactivation and activation processes.²⁹ The voltammetric experiments also reveal the global nature of isotope effects: not only is the succinate oxidation current (breaking C–H/D bonds) attenuated much more than that for fumarate reduction, but the interconversion of D-substituted substrates occurs at a higher thermodynamic potential. For a 1:1 mixture

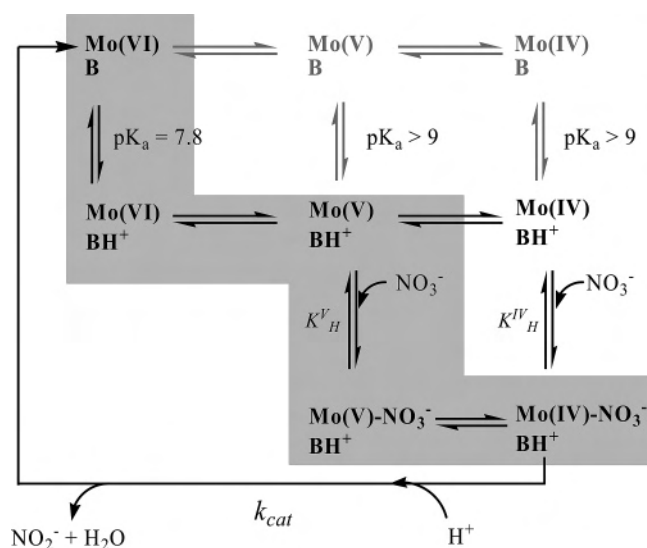
(26) Sucheta, A.; Ackrell, B. A. C.; Cochran, B.; Armstrong, F. A. *Nature* **1992**, 356, 361.

(27) Hirst, J.; Ackrell, B. A. C.; Armstrong, F. A. *J. Am. Chem. Soc.* **1997**, 119, 7434–7439.

(28) Elliott, S. J.; Léger, C.; Pershad, H. R.; Hirst, J.; Heffron, K.; Blasco, F.; Rothery, R. A.; Weiner, J. H.; Armstrong, F. A. *Biochim. Biophys. Acta* **2002**, 1555, 54–59.

(29) Limoges, B.; Savéant, J.-M. *J. Electroanal. Chem.* **2004**, 562, 43–52.

Scheme 3. Simple Catalytic Cycle for Reduction of Nitrate by Nitrate Reductase, in Which the Favored Route (Gray Background) Involves Nitrate Entering at Mo(V): Activity Thus Decreases at Negative Potentials Unless the Nitrate Concentration Is Sufficiently High to Enable Nitrate to Bind to Mo(IV)^a



of fumarate and succinate (strictly speaking, in H₂O or D₂O, as appropriate), the reduction potential of the substrate is simply the potential of zero net current.²⁷

Tunnel diode behavior has been observed for some Mo enzymes, in particular nitrate reductases from various sources.^{30,31} Figure 5B shows a set of experiments carried out on the *E. coli* enzyme NarGHI, which is normally membrane-bound but the detergent-solubilized form binds to a PGE electrode. At low nitrate concentrations, the catalytic reduction rate reaches a maximum value at approximately 0 V; then it drops as the potential is made more negative. Unlike succinate dehydrogenase, the effect diminishes as the nitrate concentration increases, suggesting that the origin lies in diminished binding affinity for nitrate as more electrons are added to the enzyme. Addition of the competitive inhibitor azide removes the effect; because this inhibitor is known to target Mo(V), we thus proposed that this oxidation state is crucial in binding nitrate.³¹ Scheme 3 depicts a catalytic cycle encompassing various reaction pathways, but the preferred route involves NO₃⁻ entering at Mo(V) rather than Mo(IV). The tunnel diode effect thus arises, because although application of a negative potential is required to drive catalytic reduction of nitrate, application of too negative a potential attenuates the rate because it forces the active site to rest predominantly in the less-active Mo(IV) state. The tunnel diode effect is very difficult to detect by conventional methods; in contrast, the PFV experiment measures activity over a continuous range of potential, easily

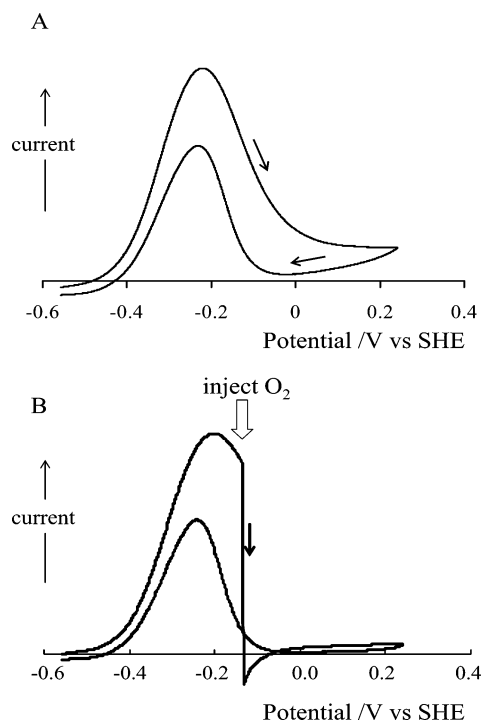


Figure 6. Voltammograms of *Allochromatium vinosum* [NiFe]-hydrogenase adsorbed on a PGE electrode, measured at low scan rates (A) under anaerobic conditions, pH 8.8, temperature = 48 °C, 1 bar H₂, electrode rotation rate = 2500 rpm, scan rate = 0.3 mV s⁻¹, and (B) with injection of O₂ during oxidative scan, pH 8.8, temperature = 45 °C, 1 bar H₂, electrode rotation rate = 2500 rpm, scan rate = 1.2 mV s⁻¹.

revealing even subtle irregularities in activity. In addition to mechanistic interest, these effects can have physiological relevance.²⁸

Tunnel diode behavior is also observed for [NiFe]-hydrogenases, and we have made detailed studies of the enzyme from *Allochromatium vinosum*. As we mentioned above, the initial observation of catalytic H₂ oxidation by this enzyme revealed only that the enzyme is very active; the chemistry was masked by diffusion control and choice of conditions that provide the simple voltammogram. We now look more closely.

An important and interesting property of hydrogenases is their inactivation under oxidizing conditions. This is revealed clearly (Figure 6A) in cyclic voltammetry of a hydrogenase film recorded as the electrode potential is cycled at a low rate (usually around 1 mV s⁻¹) between -558 and +242 mV vs SHE while the electrode is rotated rapidly in an anaerobic aqueous solution in equilibrium with 1 bar H₂.³² The limiting current plateau that is achieved at higher scan rates (>0.1 V s⁻¹) is not reached; instead, the current drops off at high potential. On the return scan, most of the activity is recovered. The catalytic current is directly related to the electrocatalytic activity of the enzyme molecules adsorbed on the electrode surface. We assume that the enzyme molecules are either active or not, in which case, a change in current corresponds to a change in the number of active enzyme molecules. The drop in current at high potential

(30) Anderson, J. L.; Richardson, D. J.; Butt, J. N. *Biochemistry* **2001**, *40*, 11294–11307.

(31) Elliott, S. J.; Hoke, K. R.; Heffron, K.; Palak, M.; Rothery, R. A.; Weiner, J. H.; Armstrong, F. A. *Biochemistry* **2004**, *43*, 799–807.

(32) Jones, A. K.; Lamle, S. E.; Pershad, H. R.; Vincent, K. A.; Albracht, S. P. J.; Armstrong, F. A. *J. Am. Chem. Soc.* **2003**, *125*, 8505.

correlates with oxidative inactivation of the enzyme observed in conventional solution studies on hydrogenases. This anaerobic switch is now quite well understood, and we return to it later.

More recently, inactivation of the [NiFe]-hydrogenase caused by direct reaction with O₂ has been examined in detail.³³ Injection of O₂-saturated buffer into the electrochemical cell solution (at a sufficiently high potential to avoid direct reduction of O₂ at the electrode) results in rapid and complete loss of electrocatalytic H₂ oxidation (Figure 6B), again consistent with solution measurements. Following removal of O₂ from solution, activity is restored on the reverse scan, with some loss that results mainly from dissociation of the enzyme from the electrode.

Potential-Step Experiments Applied to Hydrogenases.

The cyclic voltammetric experiments discussed above have been instructive in diagnosing the key features of hydrogenase inactivation/re-activation. The tiny sample requirements for PFV mean that it is feasible to carry out very extensive investigations of hydrogenases across the microbial world.³⁴ This will not only provide useful information on evolution and adaptation to aerobic environments, but hopefully also inspire catalysts for future energy technologies. Oxidative inactivation is an important limiting factor in the exploitation of hydrogenases or development of bio-inspired synthetic base-metal catalysts, and we now discuss potential-step experiments that provide more quantitative information on the rates and energetics of the reversible transformations between reduced-active and oxidized-inactive states. The essence of a potential-step experiment is that the system is perturbed by a rapid change in electrode potential; it then relaxes to a new state, and the kinetics of this process are monitored at a constant potential. Thus, to determine the true driving force dependence of a reduction process that activates an enzyme, we might set the potential at a value corresponding to a fully oxidized, inactive species and then step to different negative values to follow the kinetics of reductive activation as a function of potential.

The standard potential-step experiment is known as chronoamperometry, and this method has been widely used to study reactions of species in solution, most commonly establishing that a reaction is diffusion-controlled (in which case the current decreases as the square root of time).⁴ For adsorbed redox couples, this method is limited because the change in current is so small. However, for an enzyme, this is not so, as the current response is greatly amplified by catalytic turnover. Redox enzymes with high electrocatalytic activity such as *Allochroamatium vinosum* [NiFe]-hydrogenase ($k_{\text{cat}} \gg 1000 \text{ s}^{-1}$) are thus perfectly suited for potential-step kinetic studies. *A highly active enzyme is equivalent to an intensively colored enzyme in a spectroelectrochemical experiment.* In cases where an electrochemically triggered reaction results in change in activity of the enzyme, the rate

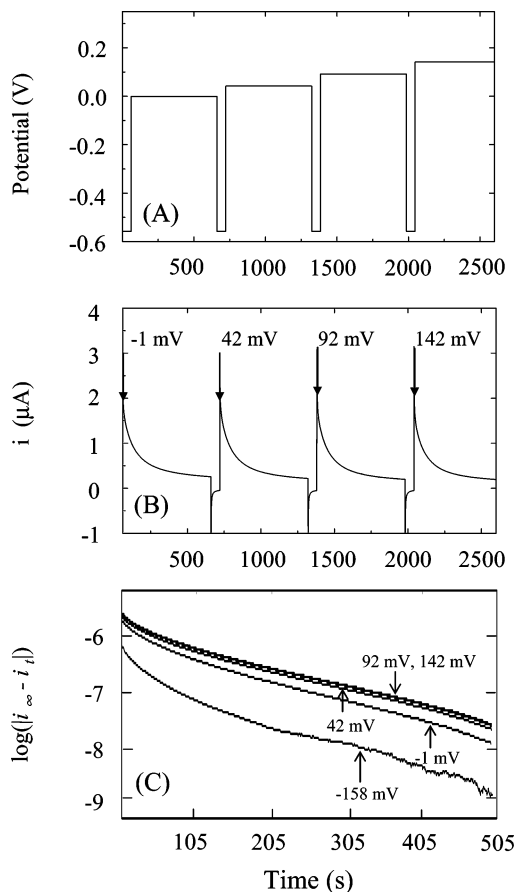


Figure 7. (A) Potential-step sequence designed to study the rate and potential dependence of oxidative inactivation of *Allochroamatium vinosum* [NiFe]-hydrogenase at a PGE electrode. (Adapted from ref 32.) (B) Current vs time profile for the potential-step sequence shown in A carried out at pH 8.8, 45 °C, 1 bar H₂ electrode rotation rate = 2500 rpm. (C) Overlay of log(current change) vs time plots for each of the inactivation steps in B, where i_{∞} is the current measured when the reaction appears to be complete and i_t is the current at time t . The trace for another experiment with a smaller driving force for inactivation (−158 mV) is also included in C.

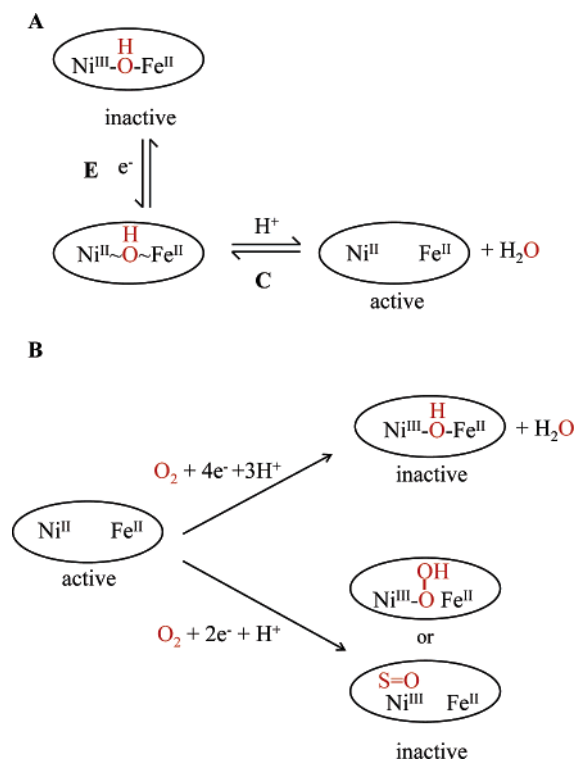
of this reaction is derived directly from the rate of change of current with time.

The series of potential-step experiments shown in Figure 7A was designed to report on the kinetics of anaerobic oxidative inactivation of [NiFe]-hydrogenase without the convolution of potential and time domains that limits the cyclic voltammetric measurements.³² The electrode was alternately poised at a high potential (−1, +42, +92, or +142 mV) to induce inactivation and then at a low potential (−558 mV) to re-activate the enzyme. These measurements were conducted at 1 bar H₂, pH 8.8, and high temperature (45 °C) to move the kinetics into a reasonable time scale. The enzyme coverage was also depleted by gentle polishing to ensure that the current was independent of electrode rotation rate and thus not controlled by H₂ mass transport. The rate of decrease of catalytic current at each potential (Figure 7B) now corresponds to the rate of hydrogenase inactivation. It is evident from the current–time profiles, and supported by the log(current change) vs time plots (Figure 7C), that the inactivation rate is independent of potential (between −158 and +142 mV). Comparisons of oxidative inactivation under

(33) Lamle, S. E.; Albracht, S. P. J.; Armstrong, F. A. J. *Am. Chem. Soc.* **2004**, 126, in press.

(34) Cammack, R.; Frey, M.; Robson, R., Eds. *Hydrogen as a Fuel: Learning from Nature*; Taylor and Francis: London, 2001.

Scheme 4. Interconversions of the Active Site of *Allochromatium vinosum* [NiFe]-hydrogenase under Anaerobic and Aerobic Conditions: (A) Anaerobic Oxidative Inactivation and Reductive Re-activation Reactions, (B) Inactivation Reactions Caused by O₂ Addition under (Top) Electron-Rich Conditions and (Bottom) Electron-Deficient Conditions



0.01 bar H₂ and at pH 7 (not shown) show that the rate is unaffected by H₂ partial pressure but is significantly lower at lower pH. The fact that the rate of oxidative inactivation is *insensitive to potential* over a range of 300 mV but *sensitive to pH* suggests that the controlling event is not an electron-transfer process, but a chemical reaction involving proton transfer. As depicted in Scheme 4A, the rate-determining step for oxidative inactivation is therefore a *chemical* (C) event rather than an *electrochemical* (E) event. This observation is important in formulation of a mechanism for oxidative inactivation and re-activation of hydrogenase, and we return to this issue shortly.

In contrast to oxidative inactivation, the rate of re-activation of anaerobically inactivated [NiFe]-hydrogenase is highly sensitive to potential, as revealed in the current vs time and log(current change) vs time plots in Figure 8.³² In each of these experiments, the adsorbed enzyme was first inactivated at high potential (not shown) before the potential was stepped down to a lower value to trigger re-activation and record the kinetics. The first 10 s of these potential-step experiments constitutes an effective dead time due to superposition of the graphite charging current on the experimental data. However, when these early data are ignored, the log(current change) vs time plots show good linearity over several half-lives consistent with a single exponential process. Rate constants for re-activation at each potential are read directly from the gradients in Figure 8B. Reductive activation is evidently a first-order process for which the rate constant increases with electrochemical driving

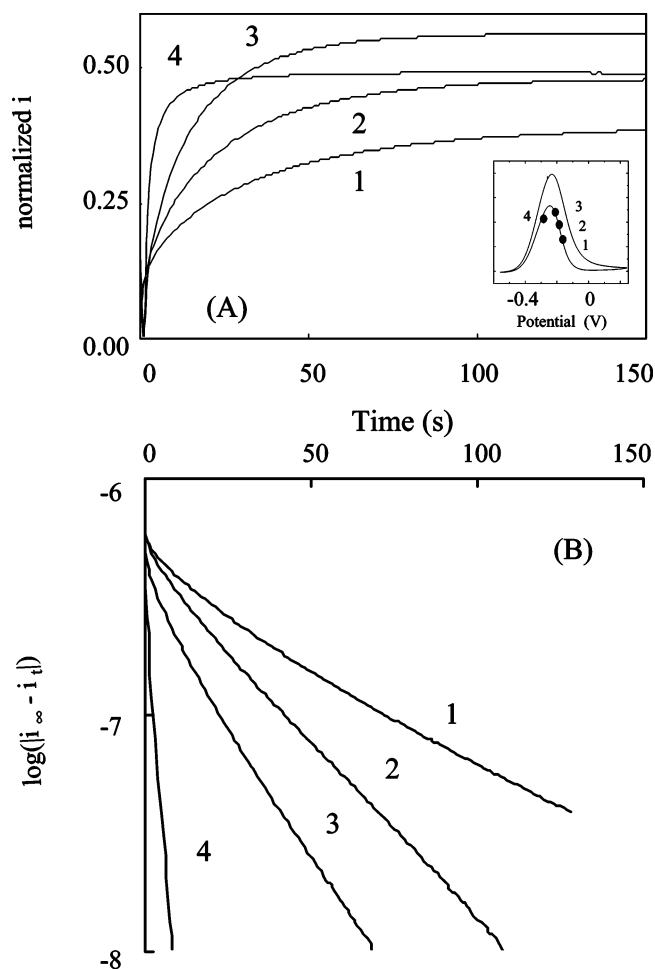


Figure 8. Potential-step experiments to measure the time course of reductive re-activation of anaerobically inactivated [NiFe]-hydrogenase as a function of potential (pH 8.8, 45 °C, electrode rotation rate = 2500 rpm, 1 bar H₂). The enzyme was first inactivated at -68 mV for 600 s (not shown), and then the potential was stepped to different values to initiate re-activation. (Adapted from ref 32.) (A) Actual data obtained for four different potential steps: 1, -168 mV; 2, -188 mV; 3, -208 mV; 4, -288 mV. To compare traces for each potential value, we normalized the amplitudes with respect to the currents measured at the beginning of the inactivation step, to compensate for slow film loss that occurs particularly at high pH. The inset shows a voltammogram measured under similar conditions indicating (●) the potentials of the reductive re-activation steps commenced from the starting potential of -68 mV and the relative current amplitude expected in each case. (B) The corresponding log(current change) vs time plots. Rate constants extracted from these data are: -168 mV, 0.021 s⁻¹ (only a guide as the line is curved); -188 mV, 0.035 s⁻¹; -208 mV, 0.052 s⁻¹. At -288 mV, the re-activation reaction is complete within the nominal dead time of the potential step.

force at potentials well below the inflection point of the rise in current (trace 1). This is consistent with a reaction that is controlled by electron transfer, i.e., the rate of reduction of Ni(III) to Ni(II) (Scheme 4A).

There is strong evidence that the active site of the anaerobically inactivated form of hydrogenase contains a hydroxide ligand in a bridging position between the Ni^{III} and Fe^{II}. Reductive activation results in reduction to Ni^{II} and loss of the hydroxide bridge. The pH and electrochemical potential dependencies of oxidative inactivation and reductive activation indicate that this reaction proceeds in two stages, where removal of the hydroxide bridge is the rate-determining step during oxidative inactivation (it is a “CE” reaction)

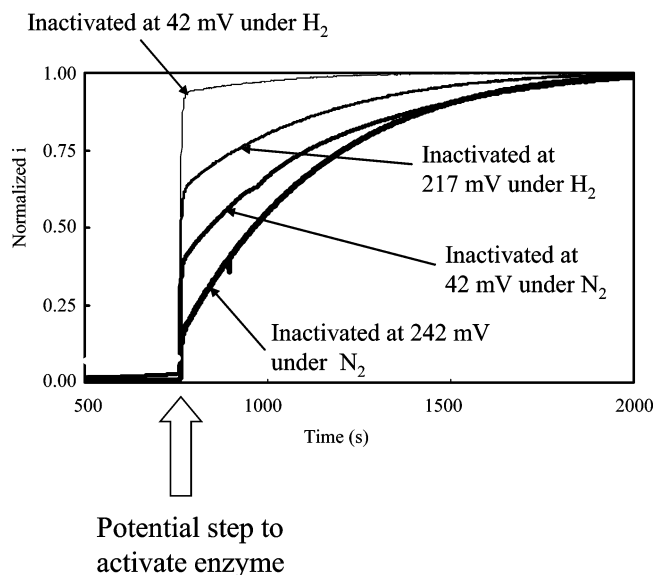


Figure 9. Current vs time traces for potential-step experiments to examine the re-activation of hydrogenase following injection of O_2 at different potentials under a N_2 or H_2 atmosphere (1 bar in either case). Initially, the electrode potential was held at -558 mV to activate the adsorbed enzyme before a potential step to the values indicated on the plot and injection of O_2 -saturated buffer. Re-activation under H_2 (1 bar) was then monitored at -158 mV after allowing time to flush O_2 from the solution. Other experimental conditions: pH 6.0, $45^\circ C$, and electrode rotation rate = 2500 rpm. (Adapted from ref 33.)

and reduction of Ni^{III} is the rate-determining step during reductive activation (an “EC” reaction). The potential-step kinetic experiments therefore permit an exquisite resolution of chemical vs electron-transfer reactions that would be difficult to obtain by other conventional solution assays, which usually involve redox dyes such as viologens as reaction partners.

The anaerobic inactivation and re-activation chemistry of the [NiFe]-hydrogenase involves only the adsorbed protein and a solvent species. A controlled potential-step study is equally useful when an additional reactant is introduced or removed during the experiment, as in the aerobic inactivation of [NiFe]-hydrogenase and its subsequent recovery when O_2 is removed.³³ Earlier reports based on conventional solution assays and spectroscopic data indicated that [NiFe]-hydrogenases are reversibly inactivated by oxygen, and further insight into this chemistry was provided by a series of carefully designed potential-step/gas-exchange experiments.

As observed in the simple cyclic voltammetric experiment shown in Figure 6B, injection of O_2 immediately results in loss of electrocatalytic hydrogen oxidation activity, but activity returns once O_2 is removed and the electrode potential is lowered. Figure 9 shows results for the reductive re-activation at -158 mV (at 1 bar H_2 , $45^\circ C$, and pH 6.0) of hydrogenase that has been subjected to injections of O_2 at different electrode potentials under either H_2 or N_2 . These experiments were performed within a sealed electrochemical cell that permits rapid exchange (ca. 5 min) of gas in the headspace above the cell solution. Whereas the reductive re-activation of anaerobically inactivated hydrogenase appears as a single, fast exponential trace (Figure 8), reductive activation of enzyme that has been inactivated by direct

reaction with O_2 proceeds in two distinct phases, demonstrating that a mixture of species has been formed. The rapidly activating phase is active within seconds, whereas the slowly activating component takes minutes to activate (half-life ca. 5 min at $45^\circ C$). The proportion of slowly activating component is much higher for experiments in which O_2 has been introduced to the enzyme under electron-poor conditions, i.e., in the absence of H_2 and at high potential.

Clearly, the reaction of *Allochroamatium vinosum* [NiFe]-hydrogenase with O_2 produces two products, each with distinct and well-defined kinetics of re-activation. The rapidly re-activating phase is favored when O_2 is added under conditions where electrons are fully available, suggesting that the formation of this species involves complete reduction of O_2 . Cyclic voltammetry shows that, when O_2 is added under these conditions (Figure 6B), the reductive re-activation peak is at a potential similar to that observed for the anaerobic inactivation/re-activation scan (Figure 6A). Furthermore, the high rate of re-activation of the rapidly activating phase is also consistent with it being the species formed under anaerobic conditions, suggesting that O_2 inactivation under electron-rich conditions leads predominantly to the species with a hydroxide bridge between active site Ni^{III} and Fe^{II} . In contrast, formation of the slowly activating phase is clearly favored by a deficiency of electrons. Thus, we tentatively assign this species to enzyme molecules that have a trapped, partially reduced O_2 molecule, such as a peroxide or oxidized cysteine (a sulfoxide $>S=O$ or sulfenic acid $-SOH$), at the active site. The two contrasting situations are depicted in Scheme 4B.

Although the aerobic inactivation reaction is triggered not by a potential step but by addition of a reactant (O_2), the precise control over potential afforded by the direct electrochemical method is crucial in dictating the outcome. Whereas EPR spectroscopic studies are able to distinguish between different species on the basis of their electronic structures, the electrochemical experiments distinguish different species on the basis of their kinetics, at a detailed level.

Conclusions

We have presented a range of examples of applications of protein film voltammetry to probe the chemistry occurring at biological redox sites and observe how catalytic activity changes in unusual ways as the electrochemical potential is varied. Potential control over a tiny sample that can be manipulated on an electrode provides a powerful advantage for many studies. High catalytic activity provides a further advantage in that it enables the kinetics of transformations between different states of an enzyme to be addressed by potential-step experiments: the signal-to-noise ratio is excellent since monitoring a highly active center is analogous to monitoring, optically, the formation or loss of a species with a high extinction coefficient. A large number of proteins have now been studied successfully as films on electrode surfaces; however, exploration of new methods for surface immobilization of proteins represents a major challenge for protein electrochemistry. Protein film voltammetry provides a unique complement to other physical methods and offers

Electrochemical Methods for Metalloenzyme Reactions

many new opportunities for discovery and exploitation of reactions of metal centers in proteins.

Acknowledgment. We are grateful to the U.K. Research Councils, EPSRC and BBSRC, for supporting these studies

over the past 10 years. Current research on hydrogenases is supported by BBSRC Grant 43/E16711.

IC048519+